WCDMA Multiclass Downlink Capacity and Interference Statistics of Cigar-Shaped Microcells in Highways

Bazil Taha Ahmed

Mosul University

bazil.taha@uam.es

Abstract: In this paper, the multiclass downlink capacity and the interference statistics of the sectors of a cigar-shaped microcells using wideband code-division multiple-access (WCDMA) with soft handover (SHO) mode are analyzed. The two-slope propagation model with log-normal shadowing is used in the analysis where a model of 8 cigar-shaped microcells is utilized. The performance of the downlink is studied for different [sector range R, standard deviation of the shadowing (σ_1 and σ_2) and propagation exponents (s_1 and s_2)]. It is found that increasing the sector range from 500m to 1000m will increase the sector downlink capacity. Also, it is found that increasing the value of the propagation parameters (σ_1 and σ_2) will reduce the downlink sector capacity. It is noticed that, the effect of changing the propagation exponent s_1 is null while increasing the propagation exponent s_2 will increase the downlink capacity.

Keywords: WCDMA, Multiclass downlink capacity, Shadowing, Soft handover (SHO) margin.

1- Introduction

CDMA cellular systems including WCDMA for UMTS employs an elaborated hand-over method in which a mobile station is simultaneously connected to several base stations. This method of hand-over is called Soft-HandOver (SHO). CDMA techniques make possible to maintain an old connection while adding a new one (make before break); however, additional resources (codes) from several Base Stations are required [1]. In downlink, this is achieved by multiple site transmission, which implies that several Base stations transmit the same signal to a certain mobile station (MS).

It is well known that, the capacity in WCDMA systems is commonly limited by interference. In order to reduce the interference level in downlink, power control techniques are proposed. Using a power control algorithm that is based on signal to interference ratio (SIR) in downlink, the power that is transmitted to the MS is adjusted to achieve the energy-per-bit to noise power spectral density ratio (E_b/N_o) requirements [1]-[2]. Therefore, more capacity can be achieved by the system if SIR-based power control techniques are used since system interferences are reduced [2].

Two issues must be taken into account in SHO performance evaluation, namely

- The active set where usual number of the involved base stations is 2 to 3.
- The SHO margin (M_{SH}) with a usual value of (3-6) dB.

The active set is the group of base stations to which a user terminal is connected. M_{SH} is the maximum allowed difference (measured in decibels) between the power that is received from the best server base stations and the power received from a candidate base station that is included in the active set of the user terminal [3].

In [4], it has been shown that SHO used in the uplink of the Mobile Telecommunications System (UMTS), reduces interference; therefore, SIR is increased. This effect is modeled as a SHO gain and can be used to offer higher quality services to users or to allocate a higher number of users in a cell (higher capacity). These analyses have demonstrated that capacity in uplink is always increased with M_{SH}. In [5], the downlink SHO performance in terms of E_b/N_o has been analyzed, assuming two candidate base stations in the active set. Connection probabilities were calculated to determine the connection situation of each mobile station location. SIR as a function of the distance to the interference base station has been given for different scenarios.

The effects of SHO on power-controlled downlink systems have been studied in [6]–[8]. In [6], Yang et al. studied the effect of cross-correlated shadowing on the SIR using hard handover and SHO algorithms. It has been demonstrated that the constant cross-correlation model overestimates the SIR in WCDMA systems. In [7], Zhang et al. obtained the downlink capacity gain for SHO CDMA systems by dividing a hexagonal layout in defined connection zones. In [8], the performance of hard and SHO algorithms in a downlink WCDMA system using a probabilistic method has been studied. The mean active set number (the average number of base stations in the active set) is calculated in a mobility scenario where the environment model is limited to the path between two base stations.

The uplink capacity of the cigar-shaped microcells in highways has been studied in [9]. In [10], the uplink capacity of WCDMA system used to service trains has been investigated. In [11], the uplink multiclass capacity is calculated for highways cigar-shaped microcells. An analytical computation of the uplink interference statistics in mobile communications has been given by [12] assuming macrocells with hexagonal grid pattern.

Downlink capacity has been studied for the case of street microcells assuming that omnidirectional antennas are used in the base stations without the use of the power control technique [13]. In [14], a class-based downlink capacity estimation of a WCDMA network has been given. Also, the downlink throughput has been given. In [15], the downlink capacity of mixed traffic in WCDMA mobile internet has been presented assuming hexagonal macrocells. In [16], the downlink capacity estimation of multi-service WCDMA cellular network has been given for voice and video services assuming a hexagonal macrocells taking into account only the expected value of the interference. No one of [14]-[16] has taken into account the effect of the interference variance on the downlink capacity.

In [17], the WCDMA worst case downlink capacity of cigar-shaped microcells using soft hand-over with SIR based power control for over-ground train service has been presented. In [17], neither the variance of the interference nor the new services incorporated by the UMTS 3.5 G standard have been considered.

In [18], the HSDPA performance in macrocells has been presented.

In [19], the performance of dual cell HSDPA has been presented assuming that users exist in macrocell environment. The results have shown that, with DC-HSDPA, realistic applications such as web browsing and video streaming see significant gains in lab as well as OTA environments compared to single cell HSDPA with or without loading due to other users. In [20], the Iub backhaul limitations with different traffic types have been analysed through simulations. User traffic data was imported from the live network in Maidenhead and used in these simulations. In [21], authors have reported the results of physical layer multiple-input–multiple-output High-Speed Downlink Packet Access (HSDPA) throughput measurements. These measurements have been carried out in two different environments, namely an alpine valley and a city. For a four transmit antenna scenario, results have been far from the optimal. In [22], a network performance comparison between HSDPA and LTE has been given. Results have shown that LTE outperforms HSDPA in terms of spectral efficiency and user

throughput. In [23], the main objective of the work was to provide an insight into the potential of HSPA+ technology as a means to enhance user experience against prior HSPA mobile broadband capabilities such as "HSDPA 7.2 and HSDPA 10.8 (SIMO 16QAM). The performance benchmark was the outcome of field tests pioneered by Vodafone, in its Vodafone Spain network, and carried out over commercial product platforms. Studied scenarios were a dense urban and a suburban ones. authors concluded that, MIMO is proving to be the most promising feature from the HSPA+ set of features with field performance in excess of expectations – in particular at cell edge. From the practical results, it has been shown that the practical peak bit rate is 75% of the theoretical peak bit rate.

The conditions that describe the rural and urban highway cigar-shaped microcells under this study are:

- The number of directional sectors of the cigar-shaped microcell is two and a directional antenna is used in each sector.
- The microcell sector has typically a range of 1 kilometer.

The main aim of this work is to investigate the WCDMA downlink capacity and interference statistics of cigar-shaped highways microcells utilizing soft handover with SIR-based power control.

The main contribution of this work is the study for the first time the effect of the interference variance and the imperfect power control on the multiclass downlink capacity of cigar-shaped microcells considering three different types of services, namely, voice, traditional data (120 Kbps) and High Speed Downlink Packet Access (HSDPA).

The rest of the paper has been organized as follows. In Section 2, the propagation model is given. In Section 3, the downlink capacity and interference statistics are analyzed. Numerical results are presented in Section 4. Finally, in Section 5 conclusions are drawn.

2- Propagation Model

In [24] , it has been shown that the two-slope propagation model is the most adequate to describe the electromagnetic waves propagation in highways. Thus the two-slope propagation model with lognormal shadowing is used in the analysis of the

downlink. The exponent of the propagation is assumed to be s_1 until the break point (R_b) and then it changes to higher value of s_2. In this way the path loss is given by:

$$L_p(dB) \approx L_b + 10s_1 \log_{10}\left(\frac{r}{R_b}\right) + L_g + \xi_1 \qquad \text{If } r \le R_b \qquad (1)$$

$$L_p(dB) \approx L_b + 10s_2 \log_{10}\left(\frac{r}{R_b}\right) + L_g + \xi_2 \qquad \text{If } r > R_b \qquad (2)$$

where L_g is the car window penetration loss, r is the distance between the microcell base station and the mobile , L_b (propagation loss at the break point) is given as:

$$L_b(dB) = 20 \log_{10}\left(\frac{4\pi}{\lambda}\right) + 10\, s_1 \log_{10}(R_b) \qquad (3)$$

The break-point distance R_b is given by [25]:

$$R_b = \frac{4h_b h_m}{\lambda} \qquad (4)$$

where

- h_b is the base station antenna height in m,
- h_m is the mobile antenna height in m,
- λ is the wavelength in m and
- ξ_1 and ξ_2 are Gaussian random variables of zero-mean and a standard deviation of σ_1 and σ_2 respectively representing the shadowing effect (path loss deviation from the average value).

Typical values of the above mentioned parameters are [9]:

- s_1 = 2.00 to 2.25,
- s_2 = 4.0 to 5.0,
- σ_1 = 3.0 to 4.0 dB,
- σ_2 = 6.0 to 8.0 dB,
- R_b = 300m,
- L_g = 4 dB.

3- Downlink Interference Analysis

Fig. 1 depicts the configuration of the 8 cigar-shaped microcells model and the coverage of each one of it. The microcells are assumed to be are regularly spaced every 2R. Thus, the sector range is R. The downlink sector multiclass capacity will be studied considering the right sector of the microcell C0. Here we will assume that users of the

right sector of microcell 0 and the users of the right sector of microcell 1 within the soft-handover zone are connected to both of the microcells (with Macrodiversity). With Macrodiversity, the SIR of the mobiles within the soft-handover zone can be improved by combining the received signals from different BS's. Therefore, the capacity can be increased in proportion to the increase in SIR [5].

If the user i is at a distance r_{io} from the microcell base station under study (C0) and at a distance r_{id} from the interfering microcell base station d as shown in Fig. 2, then the ratio of the interference signal ratio given by path loss like term $L(r_{id},r_{io})$ due to the distance only is given as:

- For the impractical case when (r_{id} and $r_{io} \le R_b$), L (r_{id} ,r_{io}) is:

$$L(r_{id}, r_{io}) = \left(\frac{r_{io}}{r_{id}}\right)^{s_1} \tag{5}$$

- If $r_{id} > R_b$ and $r_{io} \le R_b$ then L (r_{id} ,r_{io}) is given as:

$$L(r_{id}, r_{io}) = \left(\frac{r_{io}}{R_b}\right)^{s_1} \left(\frac{R_b}{r_{id}}\right)^{s_2} \tag{6}$$

- If (r_{id} and $r_{io} > R_b$) then L (r_{id},r_{io}) is:

$$L(r_{id}, r_{io}) = \left(\frac{r_{io}}{r_{id}}\right)^{s_2} \tag{7}$$

The ratio of the interference signal $L_{shd}(r_{id},r_{io})$ due to the distance and shadowing is given by:

$$L_{shd}(r_{id}, r_{io}) = 10^{(\xi_{id} - \xi_{io})/10} L(r_{id}, r_{io}) \tag{8}$$

ξ_{id} and ξ_{im} are given as

- In case of (r_{id} and $r_{io} \le R_b$), $\xi_{id} = \xi_1$ and $\xi_{io} = \xi_1$.
- If $r_{id} > R_b$ and $r_{io} \le R_b$ then $\xi_{id} = \xi_2$ and $\xi_{io} = \xi_1$.
- In case of (r_{id} and $r_{io} > R_b$), $\xi_{id} = \xi_2$ and $\xi_{io} = \xi_2$.

The received power of the desired signal is given by:

$$P_r = p_{1,i}\, 10^{-(L_{1,i}(dB) - G_{TX}(dB) - G_{RX}(dB))/10} \tag{9}$$

where $p_{1,i}$ is the transmitted power for the user at point i of the sector under study, $L_{1,i}$ is the path loss between the base station C1 and the location i measured in dB, G_{Tx} is the base station antenna gain measured in dB and G_{Rx} is the mobile antenna gain assumed to be 0 dB. In $L_{1,i}$ the effects of the distance and shadowing are included.

Equation (9) can be rewritten as:

$$P_r = \kappa\ p_{1,i} \tag{10}$$

where κ is the desired signal propagation gain.

Adapting equation (19) of reference [5] to our study case, the expected value of the intercellular interference power due to the microcells (1-7) is given by:

$$\begin{aligned} E[I_{inter}] = {} & \kappa\ p_{tm}\ \ e^{(\beta^2\sigma_c^2/2)}\ \sum_{d=2}^{7} e^{(\beta^2\sigma_{do}^2/2)}\ L(r_{id}, r_{io})\ \ Q\left[\beta\ \sigma_{do} + \frac{10\log_{10}\{L(r_{id}, r_{io})\} + M_{SH}}{\sigma_{do}}\right] \\ & - \kappa\ p_{tm}\ \ e^{(\beta^2\sigma_c^2/2)}\ \ e^{(\beta^2\sigma_{1o}^2/2)}\ \ Q\left[\beta\ \sigma_{1o} + \frac{10\log_{10}\{L(r_{i1}, r_{io})\} + M_{SH}}{\sigma_{do}}\right] \\ & + \kappa\ p_{tm}\ \ e^{(\beta^2\sigma_{1o}^2/2)}\ e^{(\beta^2\sigma_c^2/2)}\ \ Q\left[\beta\ \sigma_{1o} + \frac{10\log_{10}\{L(r_{i1}, r_{io})\} - M_{SH}}{\sigma_{do}}\right] \end{aligned} \tag{11}$$

Where

- p_{tm} is the base station total transmitted power in each direction (per sector),
- $\beta = (\ln 10)/10$,
- σ_c is the standard deviation of the power control error,
- M_{SH} is the Soft Handover margin (dB) and
- σ_{do} is standard deviation of (ξ_{id}- ξ_{io}).
- Q is the Gaussian Q function given by:

$$Q(x) = \frac{1}{\sqrt{2\pi}} \int_x^{\infty} e^{-y^2/2}\ dy \tag{12}$$

Now the general value of σ_{do}^2 is given as:

- When (r_{id} and $r_{io} \le R_b$), $\sigma_{id} = \sigma_1$, also $\sigma_{io} = \sigma_1$ then

$$\sigma_{do}^2 = 2\,(1 - C_{do})\,\sigma_1^2 \tag{13}$$

where C_{do} is the inter-sites correlation coefficient.

- If $r_{id} > R_b$ and $r_{id} \le R_b$ then the value of σ^2 is given by

$$\sigma_{do}^2 = (\sigma_2 - \sigma_1)^2 + 2\,(1 - C_{do})\,\sigma_1\ \sigma_2 \tag{14}$$

- When (r_{id} and $r_{io} > R_b$), $\sigma_{id} = \sigma_2$,, also $\sigma_{io} = \sigma_2$ then

$$\sigma_{do}^2 = 2\,(1 - C_{do})\,\sigma_2^2 \tag{15}$$

The expected value of the intracellular interference power due to base station 1 is given by:

$$E[I_{intra}] = \kappa\ \delta\ \ (p_{tm} - p_{1,i}) \tag{16}$$

where δ is the de-orthogonality factor of the order of 0.1.

Downlink power control is used to get the same SINR in all of the points of the sector under consideration. Power assigned to the user at the sector border will be the higher since it suffers from the maximum possible interference meanwhile the power assigned to the nearest user is the lower since it suffers from lower interference. The power assigned to a user at a given point is proportional to the normalized interference power (noise and interference at the point/mean value of the noise and interference at all of the sector points).

When the power control is used, the power transmitted from the base station to the desired user at location i is given by:

$$p_{1,i} \approx \frac{p_{tm}\ p_{ch}}{N_u\ \alpha} \frac{\left(I_t + P_N\right)_i}{\left(I_t + P_N\right)_{av}} \tag{17}$$

where

- p_{ch} is the ratio of the power assigned to the users ≈ 0.8 (0.2 is assigned to the pilot and common channel),
- N_u is the number of the users uniformly distributed within the microcell sector and
- α is the source activity factor (0.66 for voice and it is 1 for data).
- $(I_t+P_N)_i$ is the sum of the total effective interference and the thermal noise at point i
- $(I_t+P_N)_{av}$ is the average value of the sum of total effective interference and the thermal noise of all the users within the sector of the microcell.

From [11] and adapting the variance expression to our case, the variance of the intercellular interference power is given by:

$$\begin{aligned} \mathrm{var}\left[I_{inter}\right] = \left(\kappa\ p_{tm}\right)^2 \quad & \sum_{2=3}^{7} e^{2\left(\beta^2\sigma_{do}^2\right)}\ L\left(r_{id}, r_{io}\right)^2 \left\{ p\ g\left(\frac{r_{id}}{r_{io}}\right) - q\ f^2\left(\frac{r_{id}}{r_{io}}\right)\right\} \\ & - \left(\kappa\ p_{tm}\right)^2 \quad e^{2\left(\beta^2\sigma_{1o}^2\right)}\ \left\{ p\ a\left(\frac{r_{i1}}{r_{io}}\right) - q\ b^2\left(\frac{r_{i1}}{r_{io}}\right)\right\} \\ & + \left(\kappa\ p_{tm}\right)^2 \quad e^{2\left(\beta^2\sigma_{1o}^2\right)}\ \left\{ p\ c\left(\frac{r_{i1}}{r_{io}}\right) - q\ h^2\left(\frac{r_{i1}}{r_{io}}\right)\right\} \end{aligned} \tag{18}$$

Where

$$p = e^{2\beta^2\sigma_c^2} \tag{19}$$

$$q = e^{\beta^2\sigma_c^2} \tag{20}$$

$$g\left(\frac{r_{id}}{r_{io}}\right)=Q\left[2\beta\sigma_{do}+\frac{10\log_{10}\left\{L\left(r_{id},r_{io}\right)\right\}+M_{SH}}{\sigma_{do}}\right] \quad (21)$$

$$f\left(\frac{r_{id}}{r_{io}}\right)=Q\left[\beta\,\sigma_{do}+\frac{10\log_{10}\left\{L\left(r_{id},r_{io}\right)\right\}+M_{SH}}{\sigma_{do}}\right] \quad (22)$$

$$a\left(\frac{r_{i1}}{r_{io}}\right)=Q\left[2\beta\sigma_{1o}+\frac{10\log_{10}\left\{L\left(r_{i1},r_{io}\right)\right\}+M_{SH}}{\sigma_{1o}}\right] \quad (23)$$

$$b\left(\frac{r_{i1}}{r_{io}}\right)=Q\left[\beta\,\sigma_{1o}+\frac{10\log_{10}\left\{L\left(r_{i1},r_{io}\right)\right\}+M_{SH}}{\sigma_{1o}}\right] \quad (24)$$

$$c\left(\frac{r_{i1}}{r_{io}}\right)=Q\left[2\beta\sigma_{1o}+\frac{10\log_{10}\left\{L\left(r_{i1},r_{io}\right)\right\}-M_{SH}}{\sigma_{1o}}\right] \quad (25)$$

and

$$h\left(\frac{r_{i1}}{r_{io}}\right)=Q\left[\beta\,\sigma_{1o}+\frac{10\log_{10}\left\{L\left(r_{i1},r_{io}\right)\right\}-M_{SH}}{\sigma_{1o}}\right] \quad (26)$$

For a given outage probability P_{out}, the ratio C/I of the user under consideration is given by:

$$C/I=\frac{p_{1,i}}{E\left[I_{intra}\right]+E\left[I_{inter}\right]+\gamma\sqrt{\mathrm{var}\left[I_{inter}\right]}+P_N} \quad (27)$$

Where

- P_N is the mobile receiver thermal noise and
- γ is a parameter given by

$$\gamma=Q^{-1}\left(P_{out}\right) \quad (28)$$

with a given value of 2.06 for an outage probability of 2%. It is 2.33 for an outage probability of 1%.

The denominator of (27) represents the sum of the total effective interference (represented by the first three terms) and the mobile thermal noise.

The ratio E_b/N_o is given by:

$$E_b/N_o=G_p\,(C/I) \quad (29)$$

where G_p is the WCDMA processing gain.

For mixed services of voice and data, the ratio between the maximum transmitted power by data users and the maximum transmitted power of the voice users given in dB should be [11]:

$$\left(\frac{P_{td}}{P_{tv}}\right)_{dB} = (1+\varepsilon) \quad \left\{ G_{pv} - G_{pd} + (E_b / N_o)_d - (E_b / N_o)_v \right\} \tag{30}$$

Where

- P_{td} is the transmitted power of the data users located at the sector border,
- P_{tv} is the transmitted power of the voice users located at the sector border,
- ε is a constant with a value of 0.0 if only the mean value of the interference is considered. When the interference variance is also considered, it has a value of -0.15 to 0.15 depending on the parameters of the services under study.
- G_{pv} is the voice service processing gain in dB,
- G_{pd} is the data service processing gain in dB,
- $(E_b/N_o)_v$ is the required (E_b/N_o) for voice service given in dB and
- $(E_b/N_o)_d$ is the required (E_b/N_o) for data service given in dB.

4- Numerical Results

In this section, the WCDMA downlink capacity of the cigar-shaped microcells deployed in highways will be given. Results will include the voice service capacity, data service capacity, a combination of both and finally the HSDPA capacity.

For our calculations some reasonable figures are applied. The inter-sites correlation coefficients $C_{do} = 0.5$, $\delta = 0.1$, $s_1 = 2$, $s_2 = 4$, $\sigma_1 = 3$ dB, $\sigma_2 = 6$ dB, $\sigma_c = 1$ dB, $R_b = 300$m and R = 1000m [9] unless other values are mentioned. Also we assume the a base station total transmitted power of 1 W/sector, mobile receiver noise power of -100 dBm, an antenna gain of 12 dB and that the frequency of operation is 2.14 GHz.

In our work, downlink capacity is defined as the maximum number of simultaneous users that can be supported with an outage of 1%. **Also results are given for other outage percentage.**

Assuming that the highway consists of 6 lanes, users are generated at a space difference of 5m. At any point, depending on the distance between the user and the base station, one of the Gaussian random variables ξ1 and ξ2 is generated with a

standard deviation of σ1 and σ2 respectively. The received signal at the studied point and the interference due to the other cell is then calculated. Capacity is then calculated making a scanning of all studied point.

Firstly let us study the case of voice service assuming that $\alpha = 0.66$, $G_p = 256$ and $(E_b/N_o)_{req} = 7$ dB [11] . Fig. 3 depicts the sector downlink capacity as a function of M_{SH} for two values of the sector range R. For a sector range of 1000m, the sector downlink capacity is 142.35 voice users for M_{SH} of 0 dB meanwhile it is 182.35 voice users for M_{SH} of 3 dB. From the figure it can be noticed that, the sector downlink capacity for a sector range of 500m is lower than the sector downlink capacity for a sector range of 1000m. The same effect has been noticed for the uplink [11]. **If the outage probability is increased to 2%, capacity will be increased by 6.6%. When the outage probability is increased to 5%, capacity will be increased by 18.0%.**

Fig. 4 represents the sector downlink capacity as a function of M_{SH} for two value of s_1. It can be noticed that the downlink capacity is equal for s_1 of 2 and 2.25. Thus the inner zone of the sector related to s_1 has no effect on the downlink capacity.

Fig. 5 shows the sector downlink capacity as a function of M_{SH} for three value of s_2. It can be noticed that for s_2 of 4.5 and 5 the downlink capacity is higher that the capacity when s_2 is 4.0. This is due to the fact that, higher s_2 means higher isolation between the microcells.

Fig. 6 depicts the sector downlink capacity as a function of M_{SH} for different values of σ_1 and σ_2. It can be noticed that for higher σ_1 and σ_2, the sector downlink capacity will be lower. This is due to the increased effect of shadowing which increases the interference statistics and reduces the capacity.

The de-orthogonality factor in urban highways (with a value of 0.1) is higher than the de-orthogonality factor of rural highways (with a value of 0.05). Fig. 7 represents the sector downlink capacity as a function of M_{SH} for two different values of the de-orthogonality factor δ. It can be noticed that for higher δ, the sector downlink capacity will be lower. This is due to fact that, higher value of δ provokes higher intracellular interference and thus lower capacity.

Finally, the case of data users will be studied assuming $\alpha = 1$, $G_p = 32$ and $(E_b/N_o)_{req} = 3.0$ dB [11]. Fig. 8 portrays the sector downlink capacity as a function of M_{SH}. It can be noticed that for a sector range R of 1000 m, the downlink capacity is 29.55 data users for M_{SH} of 0 and that it increases to 37.85 data users when M_{SH} is 3 dB.

The assigned power for each of the data users should be ≈ 3.18 times the power assigned to each of the voice users. **If the outage probability is increased to 2%, capacity will be increased by 6.8%. When the outage probability is increased to 5%, capacity will be increased by 18.1%.**

Fig. 9 represents the sector downlink capacity for a mixed services (voice and data) when M_{SH} is 0 and 3 dB.

Comparing the above mentioned results with the results given by [11], it can be noticed that the uplink (with a capacity of 54.7 voice users/sector or 12.9 data users/sector) is the link that limits the sector capacity. Fig. 10 shows the downlink capacity for data users when only 33% of the base station total power is assigned to the normal users of the UMTS system. In this case, 20% of the base station total transmitted power is assigned to the common channels and 47% for the High Speed Downlink Packet Access (HSDPA) service. At M_{SH} of 1.5 dB, the downlink capacity is 66 voice users/sector or 13.65 data users/sector. Thus the downlink can support the normal users of the UMTS and the HSDPA users without being the link that limits the capacity.

In the UMTS 3.5 Generation, HSDPA service is introduced [26]. The processing gain of such service is fixed to 16. The required E_b/N_o necessary to support the minimum HSDPA modulation is 3.6 dB. In this service, power control is not used.

Let us study the downlink extra capacity of the sector assuming that many HSDPA users are incorporated to the traditional users (voice and traditional data users) of the sector. Fig. 11 shows the HSDPA extra capacity as a function of assigned power to the HSDPA service. It can be noticed that when a 47% of the sector total power is assigned to the HSDPA service, 2 HSDPA can be supported. This means that the sector downlink capacity can be 66 voice users and 2 HSDPA users or 13.65 traditional data users (with a bit rate of 120 Kbps) and 2 HSDPA users or any possible combination of the voice and data users, and 2 HSDPA users. Fig. 12 depicts the possible combinations of the sector downlink multiclass capacity.

We have to mention that, for a soft handover margin of 3 dB and s_2 of 4, only 8.6% of the users of each sector are connected to the nearest two microcells. Thus the downlink capacity increment due to the macrodiversity is marginal.

It worth mentioning that there is not any current work that deals with the same subject, thus it is not possible to compare the results of this work with other works.

5- Conclusions

In this paper, the downlink sector capacity and the interference statistics of a cigar-shaped microcells using wideband code-division multiple-access (WCDMA) with soft handover (SHO) mode have been analyzed. The two-slope propagation model with log-normal shadowing has been utilized in the analysis where a model of 8 cigar-shaped microcells has been used. The performance of the downlink has been studied for different [sector range R, standard deviation of the shadowing (σ_1 and σ_2) and propagation exponents (s_1 and s_2)]. It has been found that increasing the sector range R from 500m to 1000m will increase the sector downlink capacity. Also, it has been found that increasing the value of the propagation parameters (σ_1 and σ_2) will reduce the downlink sector capacity. It has been noticed that, the effect of changing the propagation exponent s_1 is null while increasing the value of s_2 from 4 to 5 will increase the downlink capacity. It has been concluded that reducing the orthogonality factor δ will increase the sector downlink capacity.

References

[1] H. Holma and A. Toskala, "WCDMA for UMTS," in *Radio Access for Third Generation Mobile Communications*. New York: Wiley, 2001.

[2] D. Wong and T. J. Lim, "Soft handoffs in CDMA mobile systems," *IEEEPers. Commun.*, vol. 4, no. 6, pp. 6–17, Dec. 1997.

[3] Radio Resource Control (RRC), Protocol Specification, 3GPP TSG RAN 25.331 V.5.2.0, 2002.

[4] A. J. Viterbi, A. M. Viterbi, K. S. Gilhousen, and E. Zehavi, "Soft handoff extends CDMA cell coverage and increases reverse link capacity," IEEE J. Sel. Areas Commun., vol. 12, no. 8, pp. 1281–1288, Oct. 1994.

[5] C. Mehailescu, X. Lagrange, and P. Godlewski, "Soft handover analysis in downlink UMTS WCDMA system," in Proc. IEEE MoMuC, San Diego, CA, 1999, pp. 279–285.

[6] X. Yang, S. Ghaheri-Niri, and R. G. Tafazolli, "Downlink soft handover gain in CDMA cellular network with cross-correlated shadowing," in Proc. IEEE Veh. Technol. Conf. VTC, Oct. 2001, vol. 1, pp. 276–280.

[7] D. Zhang, G. Wei, and J. Zhu, "Performance of hard and soft handover for CDMA system," in Proc. IEEE Veh. Technol. Conf. VTC, Oct. 2002, vol. 2, pp. 1143–1147.

[8] Y. Chen and L. Cuthbert, "Optimum size of soft handover zone in power controlled UMTS downlink systems," Electronics Letters, vol. 38, no. 2, pp. 89–90, Jan. 2002.

[9] B. T. Ahmed, M. C. Ramon, and, L. H. Ariet, "Capacity and Interference Statistics of Highways W-CDMA Cigar-Shaped Microcells (Uplink Analysis)", IEEE Com. Letters, Vol.6, No.5, pp 172-174, May 2002.

[10] B. T. Ahmed, M. C. Ramón and L. H. Ariet, "On the Uplink Capacity and Interference Statistics of Cigar-Shaped Road Microcells in Over-Ground Train Service", 4th IASTED International Multi-conference Wireless and Optical Communications, pp. 109-114, Bnaff, Canada, 2004.

[11] B. T. Ahmed and M. C. Ramon, "WCDMA Multiservice Uplink Capacity of Highways Cigar-Shaped Microcells", EURASIP Journal on Wireless Communications and Networking, Volume 2007, Article ID 84835, 8 pages, 2007.

[12] M. Zorzi, ”On the Analytical Computation of the interference Statistics with Application to the Performance Evaluation of Mobile Radio Systems”, IEEE Trans. Comm., Vol. 45, No. 1, pp. 103-109, January 1997.

[13] C. C. Lee and R. Steele, “CDMA for City Street Microcells “, IEE Colloquium on Spread Spectrum Techniques for Radio Communication Systems pp. 3/1-3/10, April 1993.

[14] C. Dou, and Y.H. Chang, “Class-Based Downlink Capacity Estimation of a WCDMA Network in a Multiservice Context”, Computer Communications Journal, Vol. 28, pp. 1443-1455, 2006.

[15] S. Malisuwan, “Downlink Capacity of Mixed Traffic in WCDMA Mobile Internet”, International Journal of the Computer, the Internet and Management Vol. 14, No.1, pp 1-7, 2006.

[16] F. T. Alami, N. Aknin, and A.El Moussaoui, “Capacity Estimation of Multi-Service Cellular Network, Dimensioning and Planification Network”, International Journal on Computer Science and Engineering (IJCSE), Vol. 3 No. 3, pp.1363-1368, Mar 2011.

[17] B. T. Ahmed, and M. C. Ramon, “WCDMA Downlink Capacity of Cigar-Shaped Microcells using Soft Hand-Over with SIR Based Power Control for Over-Ground Train Service”, Computer Communications Journal, Vo. 31, pp. 88-94, 2008.

[18] João Manuel Cardoso Lopes, “Performance Analysis of UMTS/HSDPA/HSUPA at the Cellular Level “, MSc. Thesis, 2008.

[19] S. Mohan, R. Kapoor and B. Mohanty, “Dual Cell HSDPA Application Performance”, VTC Spring 2011, pp. 1-6, 2011.

[20] Fourat Haider, Erol Hepsaydir, Nicola Binucci, “Performance Analysis of a Live Mobile Broadband - HSDPA Network”, VTC Spring 2011, pp. 1-5, 2011.

[21] C. Mehlführer, S. Caban, and M. Rupp, “Measurement-Based Performance Evaluation of MIMO HSDPA”, IEEE transactions on Vehicular Technology, Vol. 59, No. 9, pp. 4354 -4367, November 2010.

[22] J. Puttone, I. Repo, K. Aho, T. Nihtil, J. Kurjenniem, T. Henttonen, M. Moisio and K. Chang, “Non-regular Network Performance Comparison between HSDPA and LTE”, 2010 5th International Symposium on Wireless and Pervasive Computing (ISWPC), pp. 568-572, 2010.

[23] S. Tenorio, K. Exadaktylos, B. McWilliams, and Y. L. Pézennec, “Mobile Broadband Field Network Performance with HSPA+”, 2010 European Wireless Conference, pp. 269-273, 2010.

[24] Seungwook Min and Henry L. Bertoni “ Effect of Path Loss Model on CDMA System Design for Highway Microcells “, 48 th VTC, Ottawa, Canada, pp 1009-1013, May 1998.

[25] Ywh-Ren Tsai and Jin-Fu Chang, “ Feasibility of Adding a Personal Communications Network to an Existing Fixed-service Microwave System “, IEEE Trans. Com., Vol. 44, Nº. 1, pp 76-83, Jan. 1996.

[26] QUALCOMM, “HSDPA for Improved Downlink Data Transfer”, October 2004.

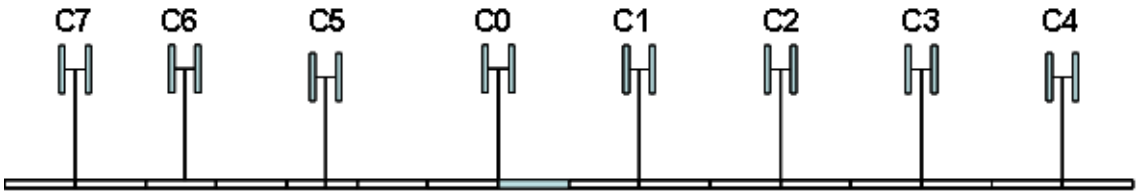

A

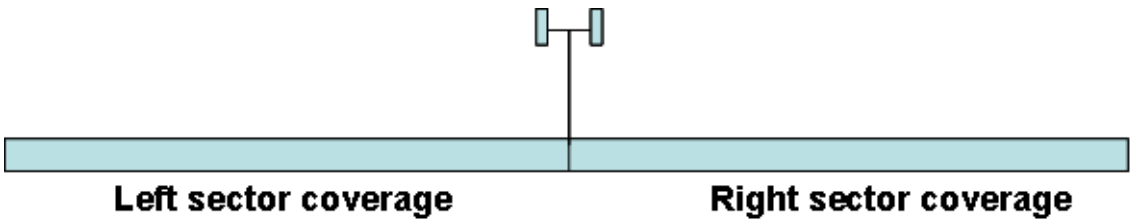

B

Fig. 1: The eight microcells model and the microcell coverage.

A- The eight cigar-shaped microcells model.

B- The microcell coverage.

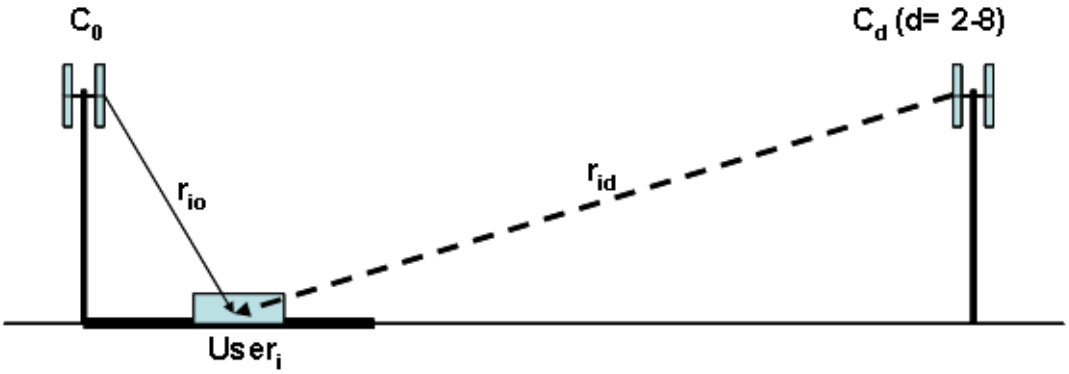

Fig. 2: Schematic diagram of microcells base stations and mobiles for highway microcells.

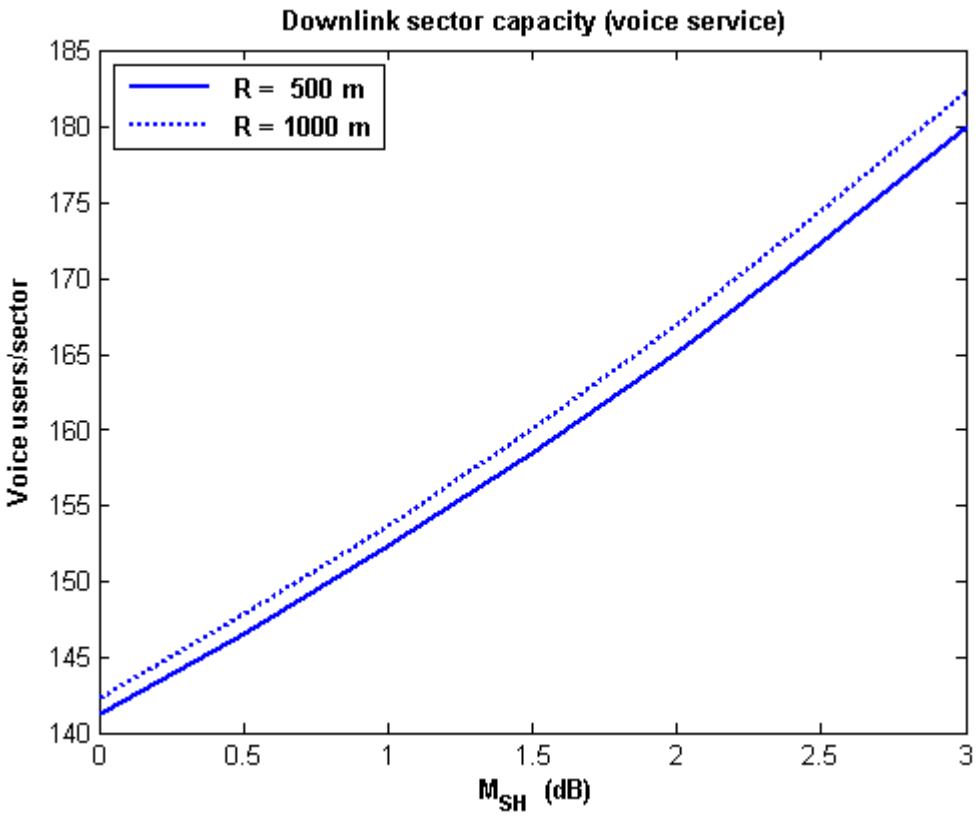

Fig. 3: Sector downlink capacity as a function of M_{SH} for two different sector range R.

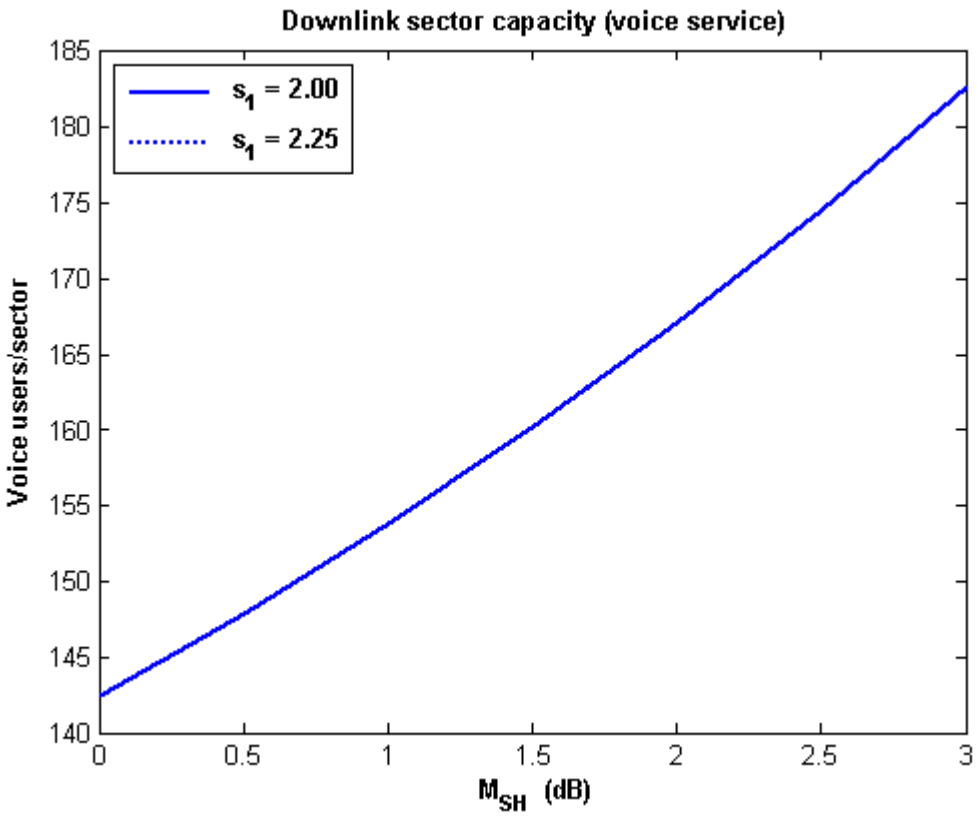

Fig. 4: Sector downlink capacity as a function of M_{SH} for two different values of s_1.

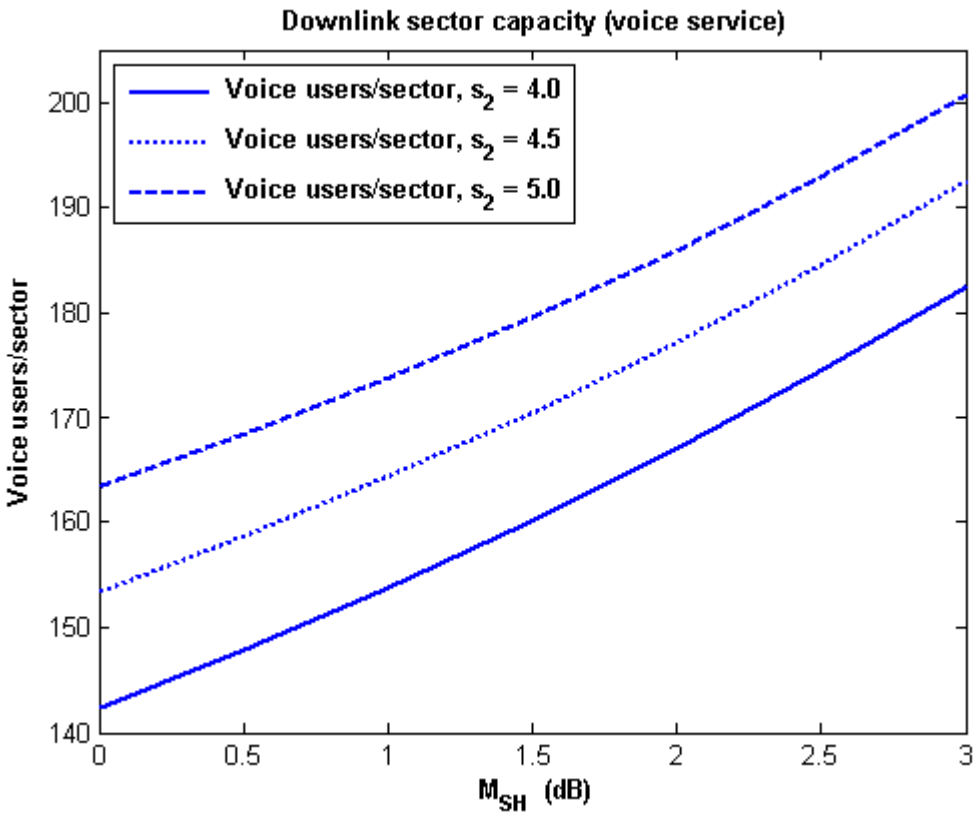

Fig. 5: Sector downlink capacity as a function of M_{SH} for three different values of s_2.

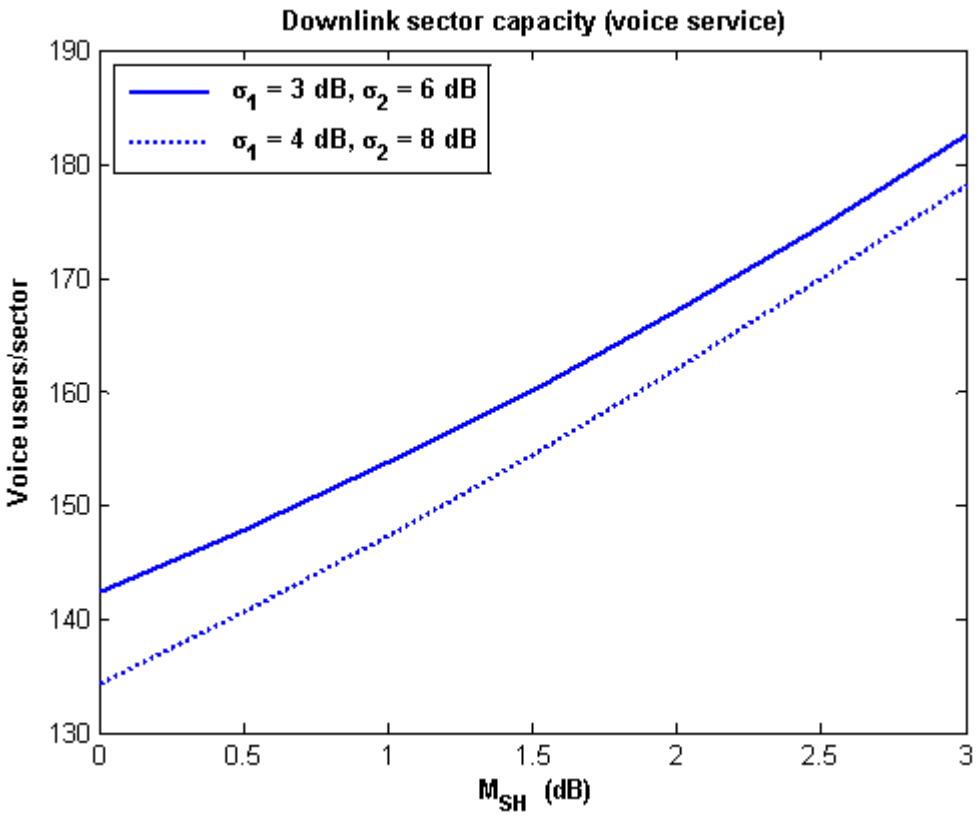

Fig. 6: Sector downlink capacity as a function of M_{SH} for different values of σ_1 and σ_2.

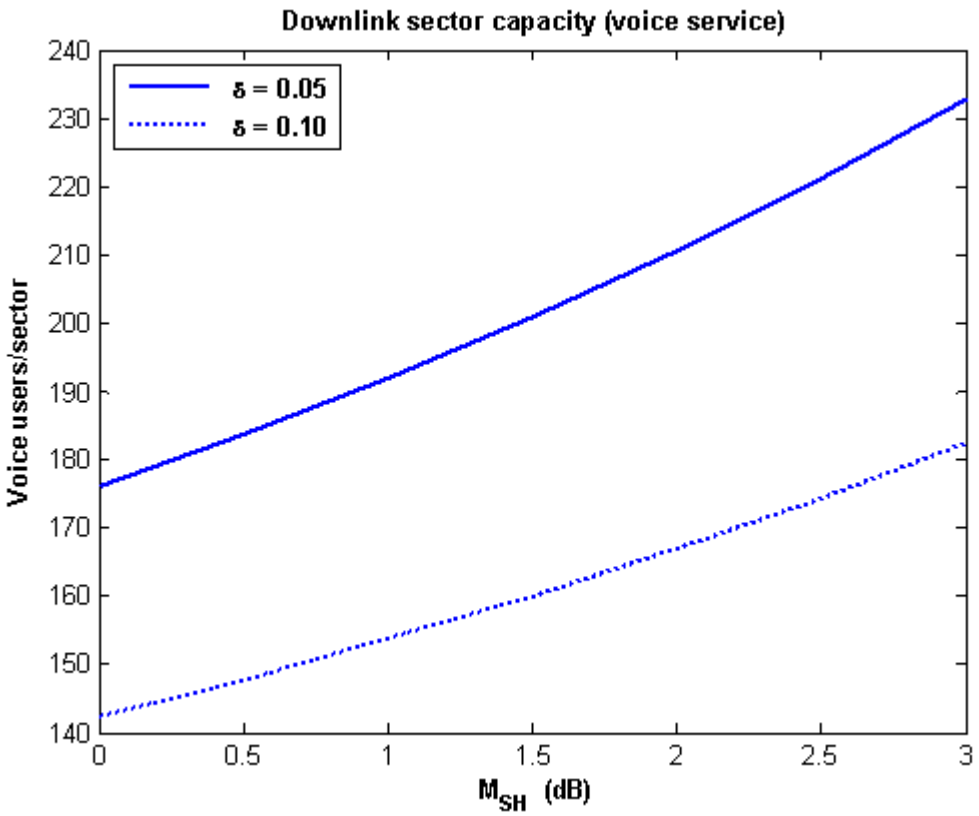

Fig. 7: Sector downlink capacity as a function of M_{SH} for two different values of the orthogonality factor δ.

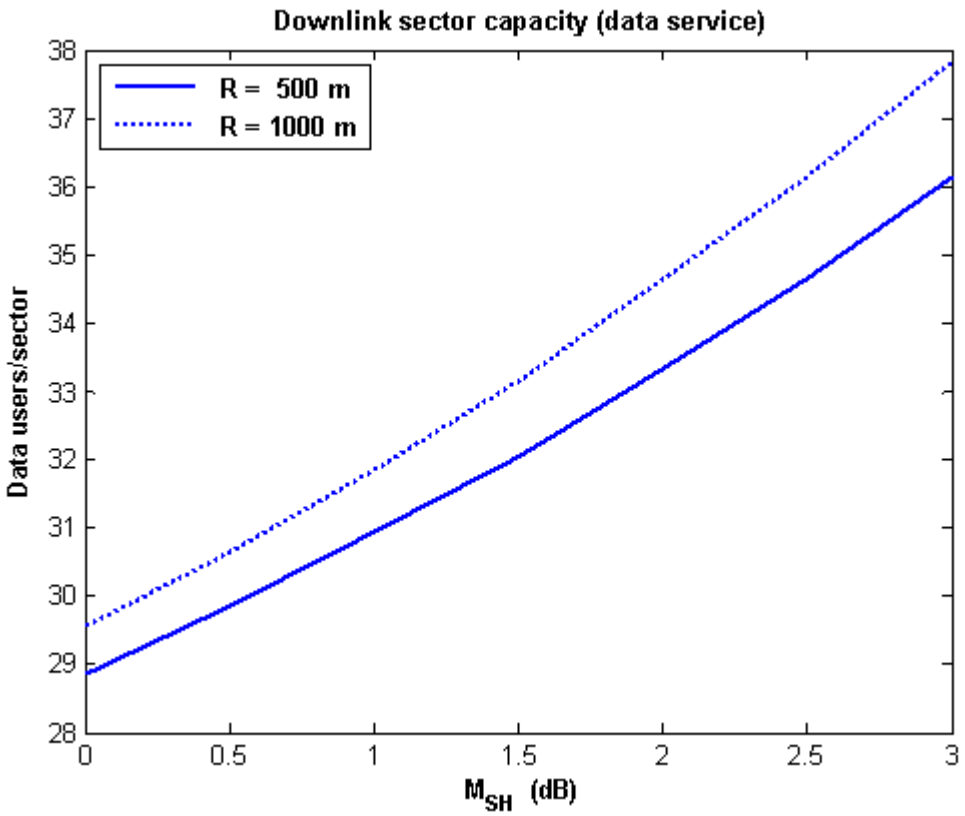

Fig. 8: Sector downlink capacity for data service as a function of M_{SH} for two values of the sector range R.

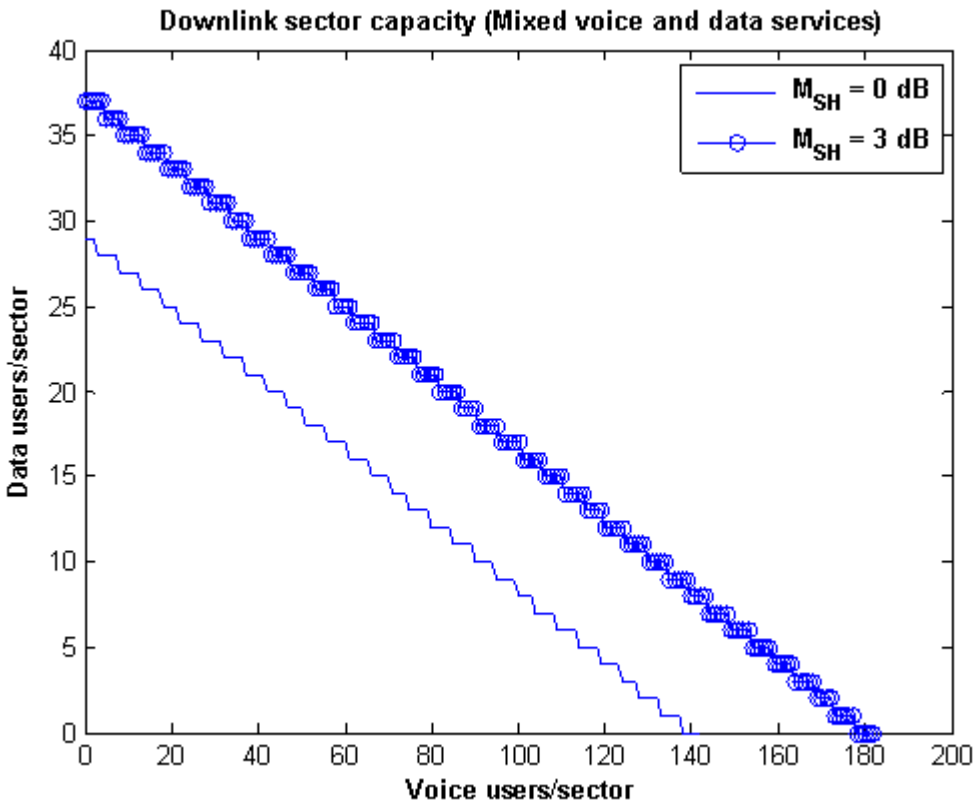

Fig. 9: Sector downlink multiclass capacity (mixed voice and data services).

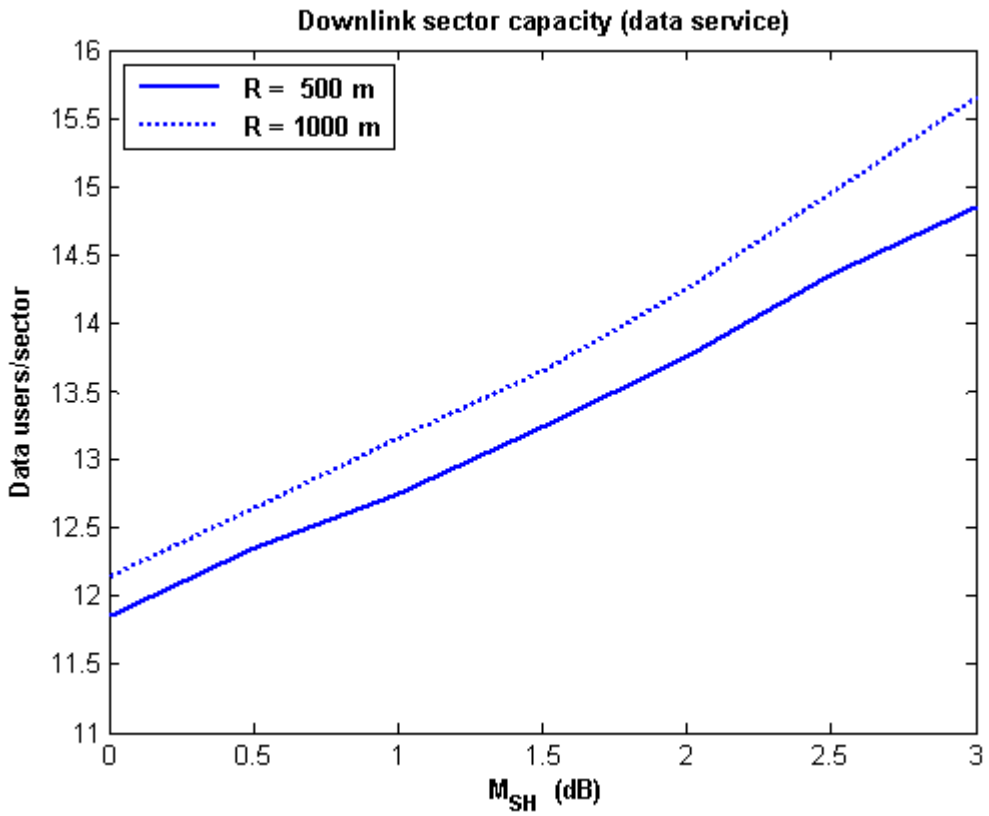

Fig. 10: Sector downlink capacity for data service as a function of M_{SH} for two values of the sector range R when only 33% of the base station total power is assigned to the normal UMTS users.

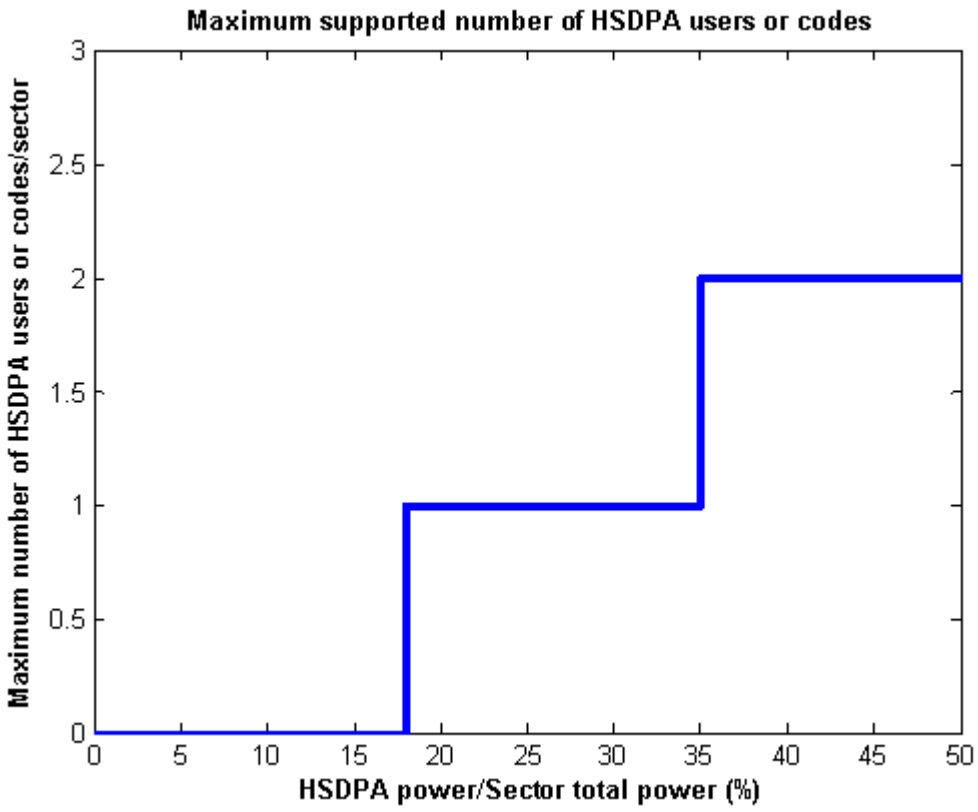

Fig. 11: HSDPA maximum supported number of users as a function of the power assigned to the HSDPA service.

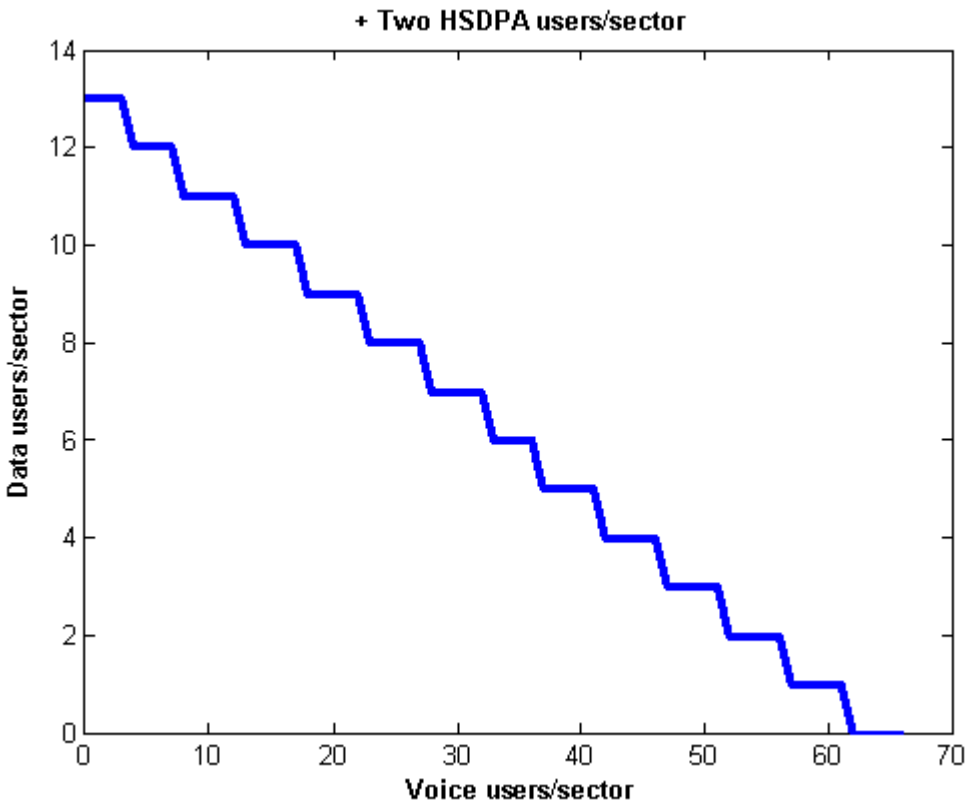

Fig. 12: Possible combinations of the downlink multiclass capacity of the sector assuming that only 33% of the sector total power is assigned to the 3G service, 47% of the sector total power is assigned to the 3.5G service and 20% of the sector total power for the pilot signal and other common channels.

*author's picture & biography
Click here to download author's picture & biography: Bazil CV+Photo.docx

Bazil Taha Ahmed was born in Mosul, Iraq, in 1960. He received the B.Sc. and M.Sc. degrees in Electronics and Telecommunication Engineering from the University of Mosul, in 1982 and 1985, respectively. He got the D. E. A. and the Ph. D degree both in Telecommunication Engineering from the Polytechnic University of Madrid in 2001 and 2003 respectively. Now he is working as an Associate Professor at the Universidad Autonoma de Madrid. He is on leaving to Mosul University. He has published more than 100 scientific journal and conference papers in the area of the electromagnetic propagation and CDMA systems, particularly the CDMA capacity. His research interests include CDMA Capacity and Radiocommunication Systems Coexistence.